

Hydrophobic superparamagnetic FePt nanoparticles in hydrophilic poly(*N*-vinylcaprolactam microgels: a new multifunctional hybrid system

Katharina Wiemer^{1§}, Karla Dörmbach^{2§}, Ioana Slabu³, Garima Agrawal², Tobias Caumanns⁴,
Svenja Danielle Marie Bourone¹, Joachim Mayer⁴, Julia Steitz⁵, Ulrich Simon¹, Andrij Pich^{2*}

¹ Institute of Inorganic Chemistry, RWTH Aachen University and JARA-Soft Matter Science,
Landoltweg 1, 52074 Aachen, Germany

² DWI-Leibniz Institute for Interactive Materials e.V. and Institute for Technical and
Macromolecular Chemistry, RWTH Aachen University, Forckenbeckstraße 50, 52056 Aachen,
Germany

³ Physikalisch-Technische Bundesanstalt, Berlin, Germany.

⁴ Central Facility for Electron Microscopy, RWTH Aachen University, Ahornstrasse 55, 52074
Aachen, Germany.

⁵ Institute for Laboratory Animal Science, University Hospital RWTH Aachen University,
Pauwelsstraße 30, 52074 Aachen, Germany

§Authors have equally contributed

*Correspondence author - pich@dwi.rwth-aachen.de

Supporting Information

Transmission profile

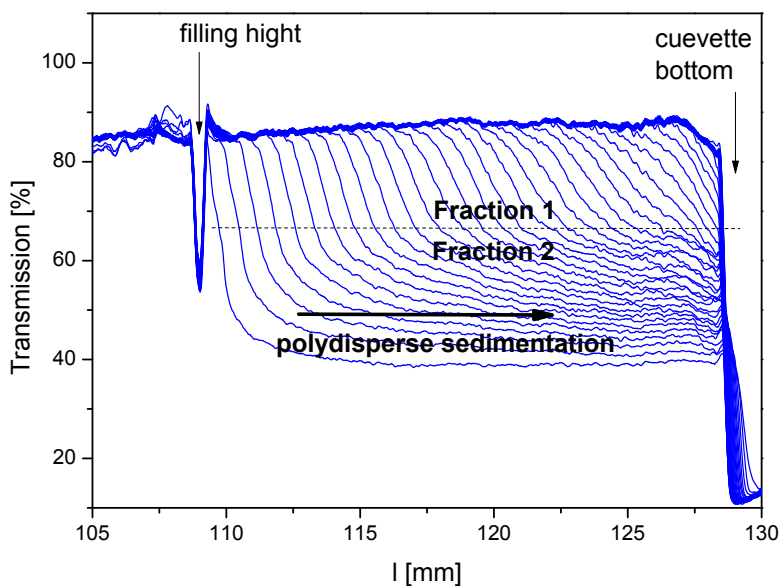


Figure S11. Transmission profiles for sample MG@FePt-3 for determination of sedimentation behavior.

For sample MG@FePt-3 transmission profiles are displayed exemplarily for all samples. Figure S11 shows the polydisperse sedimentation towards the cuvette bottom. Obviously two fractions were detected. The dash line is indicating the border between the fractions. The first fraction, upper part of the graph, consisted of slowly settling particles. In the second fraction the particles settled much faster. We assume that the first fraction consists of well-dispersed hybrid microgels, while the second fraction might consist of highly loaded or slightly agglomerated hybrid microgels.

Table S11. Sedimentation velocity for FePt loaded microgel samples (centrifugation speed: 1,111 rcf, temperature: 20°C)

Sample	$V_{\text{sed, fra1}}$ [$\mu\text{m} \cdot \text{s}^{-1}$]	$V_{\text{sed, fra2}}$ [$\mu\text{m} \cdot \text{s}^{-1}$]
MG (reference)	2.33 ± 0.01	-
MG@FePt-1	2.60 ± 0.02	5.58 ± 0.19
MG@FePt-2	2.72 ± 0.01	4.53 ± 0.09
MG@FePt-3	3.28 ± 0.01	6.89 ± 0.29
MG@FePt-4	3.27 ± 0.01	15.08 ± 0.60
MG@FePt-5	3.37 ± 0.04	30.36 ± 1.42

Table S12. Amounts of microgel and FePt nanoparticles for hybrid nanoparticle preparation

Sample	MG [mg]	FePt [mg]	MG [mL]	FePt [μL] ^[a]
MG@FePt-1	54.0	0.54	5	54
MG@FePt-2	54.0	1.08	5	108
MG@FePt-3	54.0	2.70	5	270
MG@FePt-4	54.0	4.05	5	97
MG@FePt-5	54.0	5.4	5	130

[a] The used dispersions of FePt nanoparticles were used from the same batch, but concentration of dispersion was varied.

XRD of fcc FePt NPs

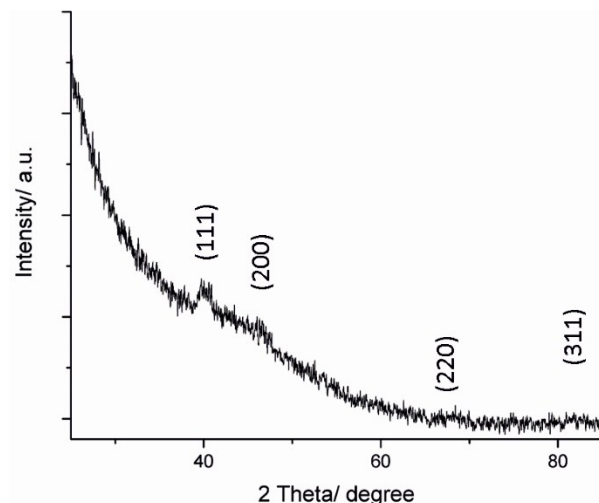


Figure SI 2: XRD of FePt NPs at room temperature.

IRRAS measurements of MG@FePt

In order to determine the bonding characteristics of the FePt NPs in the microgels, different samples, namely pure MG, pure FePt NPs and MG@FePt were analyzed by means of Infrared Reflection Absorption Spectroscopy (IRRAS). We decided to characterize the hybrid microgels by means of IRRAS so as to retain the colloids in their natural swollen state, instead of freeze drying them and measuring them as KBr pellet. On top of that advantage, IRRAS presents an increased signal intensity as compared to traditional IR measurements performed in transmission due to the fact that the samples are immobilized on a metallic surface.^[1] This enhanced signal is crucial to detect the relatively low amount of ligand molecules on the FePt NPs incorporated in the MG as compared to the abundance of functional groups composing the MG themselves. In order to deposit the MG and FePt NPs as a monolayer or possibly as a thin multilayer a droplet of each sample was

drop-cast on a platinum substrate and incubated for 45 min. Thereafter, the remaining dispersion was removed and the substrate thoroughly rinsed.

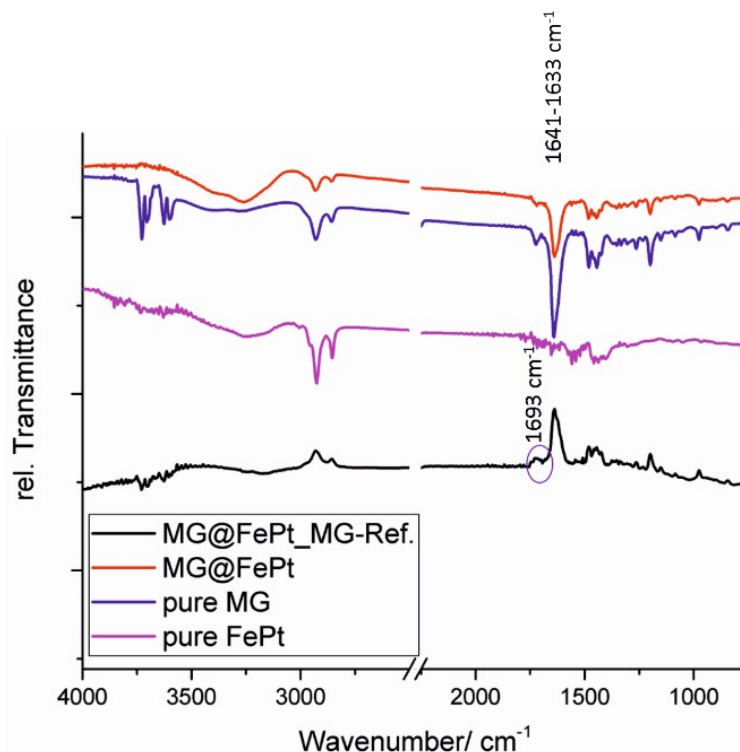
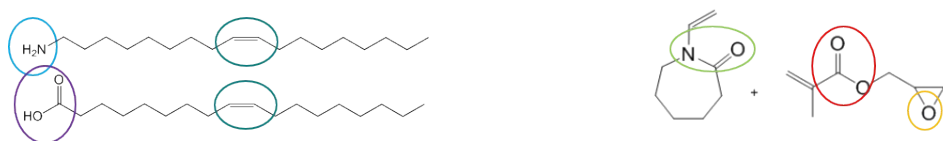


Figure SI 3: IR Spectra of the samples MG@FePt_MG-ref., MG@FePt, pure MG and pure FePt NPs.

In Figure SI 3 the respective IRRAS spectra are shown. Apart from performing IRRAS measurements during which a pristine platinum substrate was used as reference, we also conducted IRRAS measurements of MG@FePt for which the sample of pure MG was applied as reference (MG@FePt_ref.MG). The strong peak at 1641-1638 cm⁻¹ can be attributed to the amide group of the microgel. In Table SI 3 an overview of the characteristic group frequencies of the FePt NPs' ligands and of the microgels' monomers is given.

Table SI 3: Characteristic group frequencies of the FePt NPs stabilizing ligands as well as of the microgels' monomers.



FePt ligands characteristic Groups	Wavenumber/ cm^{-1}	MG characteristic groups	Wavenumber/ cm^{-1}
Amine group (oleylamine)	$\nu(\text{NH}_2)$ 1577	Ester group	$\nu(\text{C-O-C})$ 1200 $\nu(\text{C=O})$ 1719-1724
Carboxylic acid (oleic acid)	$\nu_s(\text{COO}^-)$ 1558 $\nu(\text{C=O})$ 1693-1697	Ether group	$\nu(\text{HC-O-CH}_2)$ 1085
Double bonds	$\nu(\text{C=C})$ 1653	Amide group	$\nu(\text{N-C=O})$ 1641-1638

Details of the recorded IRRAS spectra are shown in Figure SI4. The black curve corresponds to the spectrum of the MG@FePt sample recorded using the MG sample as reference. The peaks arising from the characteristic groups contained in the microgels are reversed due to the fact that the concentration of the microgels in the reference sample exceeded that in the MG@FePt sample. However, a single peak at 1693 cm^{-1} is not inverted and can be unambiguously assigned to the carbonyl stretching vibration ($\nu(\text{C=O})$) of the oleic acid ligand (see also Table SI 3), revealing that its acidic groups are not deprotonated which is consistent with the pH of 4.5 adjusted during the loading of the microgels with FePt NPs. Characteristic vibration frequencies arising from oleylamine, such as $\nu(\text{NH}_2)$, were not detected, since they do not absorb as strongly as $\nu(\text{C=O})$ ^[2] and are therefore in all likelihood overlapped by peaks of the microgels' characteristic groups.

Hence, the IRRAS measurements showed that along with the FePt NPs the ligands stabilizing those are introduced into the microgels. Furthermore, the applied solvent strongly affects the bonding characteristics between the FePt NPs and the stabilizing oleic acid ligand.

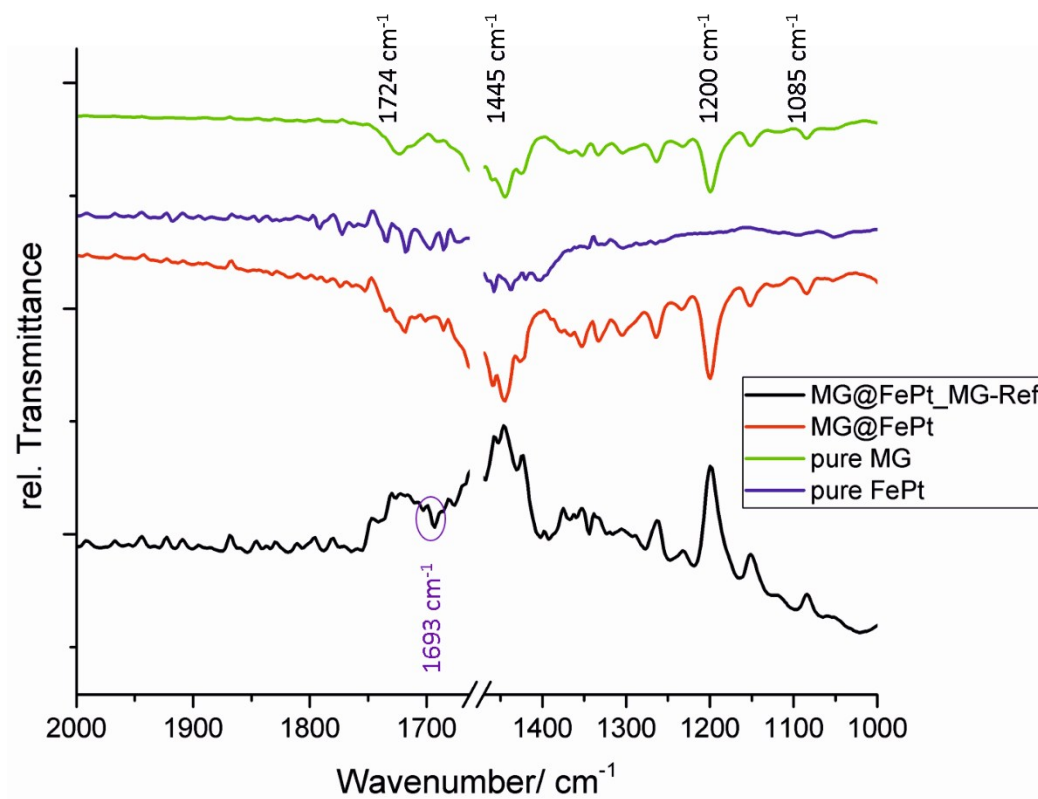


Figure SI 4: IR Spectra of the samples MG@FePt_MG-ref., MG@FePt, pure MG and pure FePt NPs in the range between 1000 and 2000 cm⁻¹.

Coercitivity and remanence magnetization values of FePt NPs and MG@FePt

For a better visualization of the difference between the magnetization values of hybrids and pristine FePt especially at low fields, a logarithmic representation of the magnetization curves is shown in Figure SI 5.

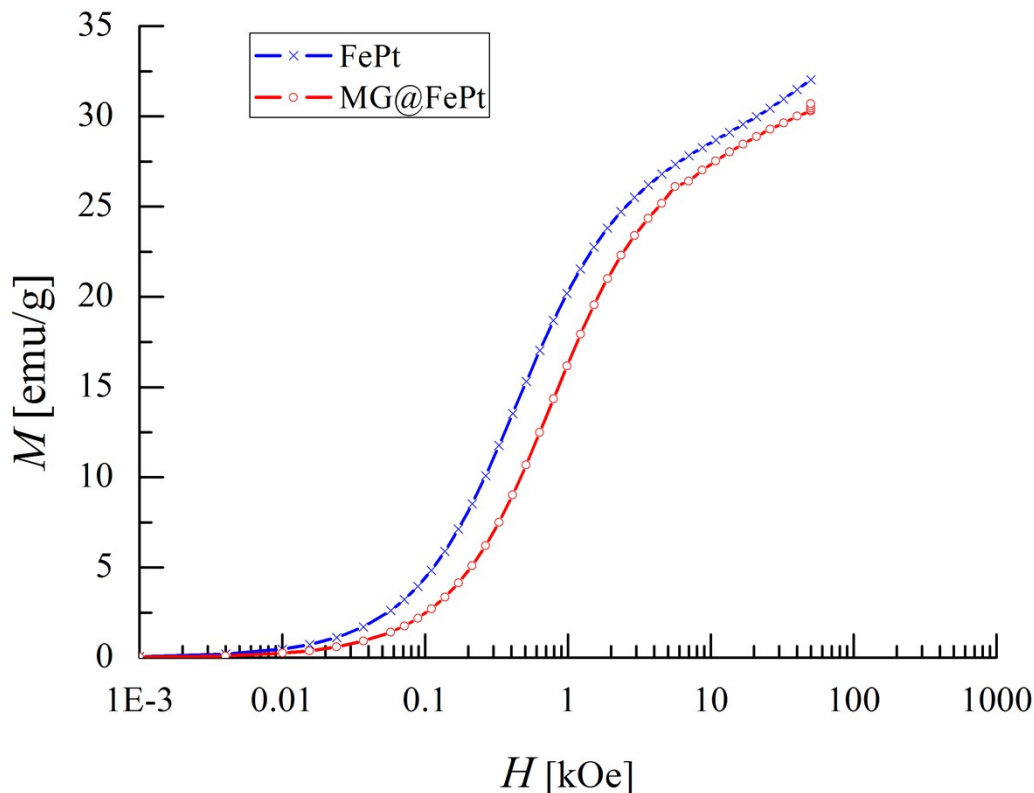


Figure SI 5: Magnetization curves for dried FePt NPs and FePt NPs inside the microgels (logarithmic scale).

For the determination of the coercitivity and remanence magnetization values, magnetization measurements were performed at 295 K varying the field strength from - 30 kOe to 30 kOe. The results are shown in table SI 4 and Figure SI 6.

Table SI 4: Coercivities and reduced remanences at room temperature.

Sample	Coercivity H_c [Oe]	Reduced remanences (Mr/Ms)
FePt	7.74	0.05
MG@FePt-5	7.47	0.02

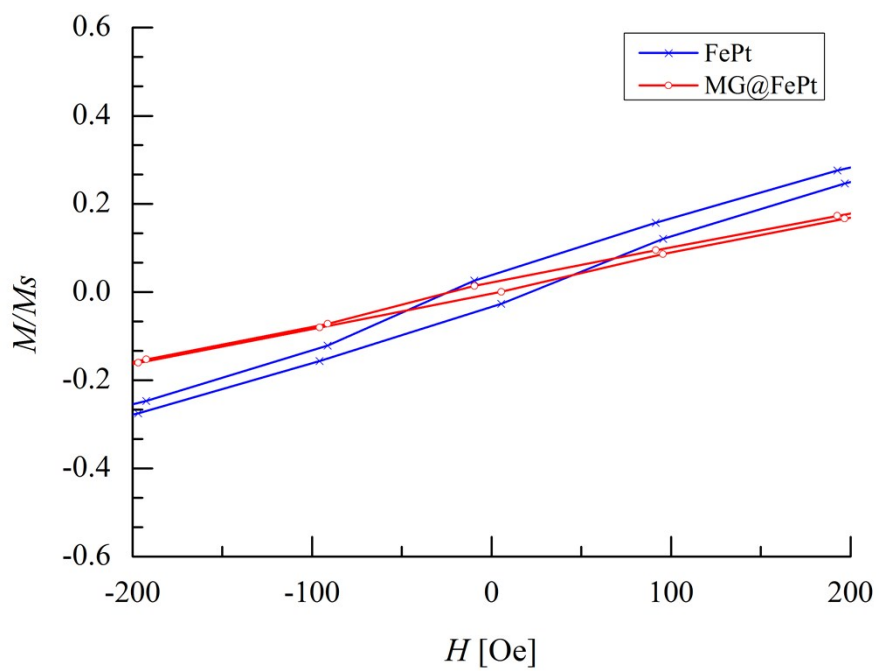


Figure SI 6: Magnetization curves for dried FePt NPs and FePt NPs inside the microgels showing coercivities and reduced remanences at room temperature.

XRD of fcc FePt with different temperatures

The respective XRD patterns are displayed in Figure SI 7. A room temperature measurement of the FePt NPs indicates that the FePt NPs are in the anticipated fcc structure. With rising temperature up to 500 °C a change in crystallinity is observed accompanied by the transformation from the fcc phase to the fct phase. This is most obviously indicated by an additional (110) reflex, which is consistent with literature.^[3,4]

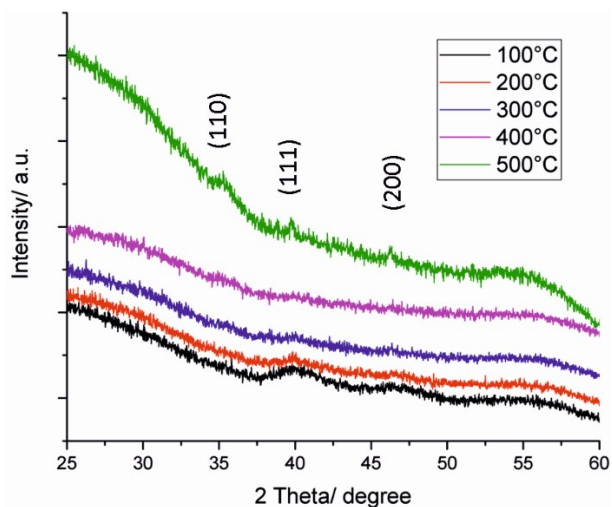


Figure SI 7: XRD patterns of FePt NPs with increasing temperature.

TGA measurements of the microgel and microgel FePt hybrids

TGA measurements for the microgels before and after loading of FePt nanoparticles are shown in Figure SI 8. Several samples (pure microgel, microgels with 1 wt.% and 7.5 wt.-% FePt NPs loading) were analyzed regarding their mass loss up to 650 °C and no significant change in mass loss/gain was observed above 500°C as indicated by the plateaus reached at this temperature. Based on these findings other microgel samples were heated up to 500°C for the determination of FePt NPs loading.

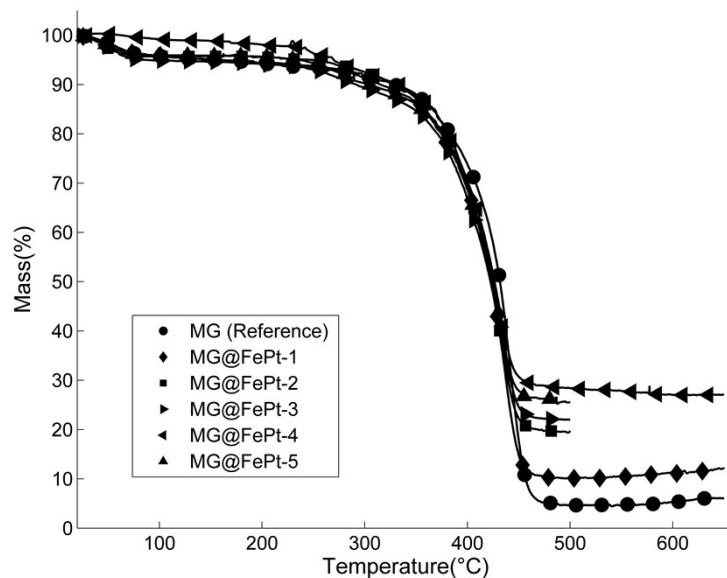


Figure SI 8: TGA measurements of microgel (reference) and microgels with different FePt NPs loading degrees.

- [1] R. G. Greenler; "Infrared Study of Adsorbed Molecules on Metal Surfaces by Reflection Techniques", *J. Chem. Phys.* **1966**, *44*, 310-315.
- [2] G. Socrates; "Infrared and Raman Characteristic Group Frequencies", John Wiley & Sons, Chichester 2001.
- [3] A. Balaceanu, D. E. Demco, M. Möller, A. Pich, *Macromolecules*, 2011, *44* (7).
- [4] H. Loc Nguyen, L. E. M. Howard, G. W. Stinton, S. R. Giblin, B. K. Tanner, I. Terry, A. K. Hughes, I. M. Ross, A. Serres, J. S. O. Evans, *Chem. Mater.* 2006, **18**, 6414-6424.
- [5] S. Sun, C. B. Murray, D. Weller, L. Folks, A. Moser, *Science*, 2000, **287**, 1989-1992.